

# HYPERVELOCITY IMPACT TESTING OF CFRP/AL HONEYCOMB SATELLITE STRUCTURES

Frank Schäfer<sup>(1)</sup>, Roberto Destefanis<sup>(2)</sup>, Shannon Ryan<sup>(1)</sup>, Werner Riedel<sup>(1)</sup>, Michel Lambert<sup>(3)</sup>

<sup>(1)</sup> Fraunhofer EMI (Ernst-Mach Institut), Eckerstraße 4, 79104 Freiburg, Germany,  
Email: schaefer@emi.fhg.de, ryan@emi.fhg.de, riedel@emi.fhg.de

<sup>(2)</sup> Alenia Spazio S.p.A., Str. Antica di Collegno 253, 10146 Turin, Italy, Email: roberto.destefanis@aleniaspazio.it

<sup>(3)</sup> ESA-ESTEC, Postbus 299, NL-2200 AG Noordwijk, The Netherlands, Email: michel.lambert@esa.int

## ABSTRACT

In this paper, ballistic limit tests on 5 different Carbon-fibre Reinforced (CFRP) Honeycomb (H/C) sandwich panels (SP) are reported. The CFRP H/C SPs presented are typical for application in various current satellite structures. Conductivity measurements of the downrange fragment cloud have been made using electrodes that were mounted on the witness plate. It was found that the fragment cloud acts as a conductive medium between the electrodes, enabling current flows across the electrodes of several tens of milli-amperes with duration of a few milliseconds. Initial impact tests on harnesses behind CFRP H/C SP have been performed. The harnesses consisted of two circuits that were operated at different voltages (28 V and 50V). Besides severe impact damage to the cables, leakage currents between the circuits have been observed. Additionally, large peak voltages in the electrical circuits during hypervelocity impact have been measured.

## 1. INTRODUCTION

The rapidly increasing number of space debris particles in Earth orbit makes the need for analysis of hypervelocity impact on spacecraft structures apparent. Composite honeycomb Sandwich Panels (SPs), consisting of face sheets of CFRP with Aluminium H/C cores, are among the most commonly used structures for satellites due to the enhanced structural benefits they provide.

One important limitation of CFRP H/C SP structures is their poor hypervelocity impact protection performance (a result of their low deformability and energy absorption capacity). Few studies have looked at the ballistic limit performance of these structures and the secondary effects on internal spacecraft components upon exceeding these ballistic limits. Besides mechanical damage to components, the downrange ejection of conductive carbon fibers leads to contamination of the satellite interior and increases the risk of electrical interactions with electronic components.

## 2. OVERVIEW OF THE TEST PROGRAM

The test program consists of hypervelocity impact tests on a variety of CFRP H/C sandwich panels, planned for investigating both the ballistic limit conditions of the panels at selected impact angles and the various effects related to downrange ejection of fragments upon perforation of the sandwich panels (i. e., the mechanical damages and electrical interferences induced inside the satellite). The latter test set-ups consisted of witness plates simulating the housing of electronic equipment, located downrange from the SP structure. To capture any possible electrical interference inside the spacecraft caused by the fragment cloud (consisting of conductive fibers), the witness plates contained spaced electrodes, which were fed with an electrical voltage typical for satellites (28 V). These tests will be referred to as “cloud conductivity measurement tests”. The other major investigative goal of the program, the vulnerability of harness routed inside the satellite, was achieved via a set-up consisting of harness mounted on the witness plates. The harness was operated during impact such that one half of the twisted pair cables carried current from a 28 V power source, while the other half carried current from a 50 V power source. These tests will be referred to as “harness impact tests”. The projectiles were all Al spheres. Projectiles up to 1.25 mm in diameter were from Al 2017 T4 alloy. Larger diameter projectiles were from unalloyed aluminum (Al 99.98%).

The impact test campaign is ongoing. Hence, this paper contains only a selection of data available at the time of publication. All analysis is preliminary.

### 2.1 Test Samples

The CFRP H/C SPs used in the impact test campaign were selected according to their relevance in spacecraft applications and their availability. The sandwich panels used (and described in the following), are from RADARSAT2, GOCE, and BEPPO-SAX missions.

Three different CFRP H/C SP structures were available from the RADARSAT2 satellite: shear panels, cone panels, and +/-Z platforms. All panel FS consisted of a number of stacked HYE 4934C K139 unidirectional

fiber plies (FL02), with outer layers of HMF196/34 T300-1k fabric (FL01). The face-sheets all had a density of  $1.80 \text{ g/cm}^3$  and a fibre volume content of 60%. The H/C core for all three panels was Al 3/16-5056-.001P. The three different structures will be referred to as: cone panels (RAD3), shear panels (RAD2), +/-Z platforms (RAD1).

The RAD1 structure (Areal Weight  $AW = 0.7017 \text{ g/cm}^2$ ) consisted of 1.13mm thick, quasi-orthotropic ( $0, \pm 45, 90$ ) face-sheets (9 layers) with a 50.8 mm thick Al H/C core. RAD2 ( $AW = 0.5847 \text{ g/cm}^2$ ) had 1.25 mm thick, quasi-orthotropic ( $0, \pm 45, 90$ ) face-sheets (10 layers) with a 25.4 mm thick Al H/C core. RAD3 ( $AW = 0.4217 \text{ g/cm}^2$ ) was constructed from 1.25 mm thick, load-oriented ( $0, \pm 9$ ) face-sheets (10 layers), with a 12.7 mm thick H/C core.

The GOCE structure panels ( $AW = 0.7807 \text{ g/cm}^2$ ) consisted of 2.0mm thick, quasi-orthotropic ( $0, \pm 45$ ) face-sheets from 16 layers of M/18/32%/M55J/145 u.d. ply. The laminates had a density of  $1.65 \text{ g/cm}^3$  and a fibre volume content of 60%. The Al H/C core had a thickness of 11mm (specification: 3/16-5056-.001P).

The BEPPO-SAX structure panels ( $AW = 0.4405 \text{ g/cm}^2$ ) were made 0.75mm thick, load-oriented ( $0, \pm 60$ ) face-sheets from 6 layers of NCHM 14/34%137/6K/M40B u.d. ply. The laminates had a density of  $1.6 \text{ g/cm}^3$  and a fibre volume content of 60%. The Al H/C core had a thickness of 31.5 mm (specification: 3/16-5056-0.001P).

## 2.2 Test Set-ups

For the ballistic limit tests of CFRP H/C SP, witness plates were placed 100 mm behind the panels. The 0.5 mm thick WPs were from Al 2024 T3.

The set-up for the cloud conductivity measurement tests consisted of 1.5 mm thick WPs (300 mm x 300 mm size) from Al 7075 placed 100 mm behind the panels. The electrodes were made from 1.0 mm thick copper, having a length of 300 mm and a width of 10 mm (Fig. 2). The electrodes were mounted perpendicularly on the WPs via fixation blocs, and spaced at 100 mm (centred). The electrodes were additionally separated from the WPs by ca. 2 mm to avoid electrical contact. During impact testing, a constant voltage of 28 V was

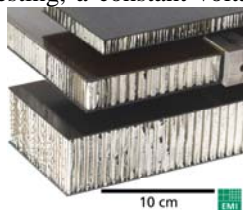


Figure 1. RADARSAT2 CFRP H/C SP (RAD1,RAD2,RAD3)

fed to the electrodes. Current flow across the electrodes was monitored by a load resistor that was connected in parallel to a digital oscilloscope.

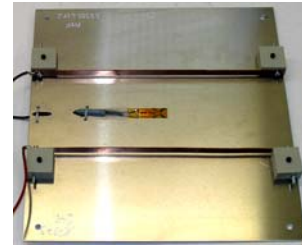


Figure 2. Electrode set-up for cloud conductivity measurements (with piezofilm stress gauge mounted in the center)

For the harness impact tests the same witness plate was selected as for the electrode impact tests. The cables (type: Raychem 55A0124-20-9/9) were operated during impact, having a consumer (resistor) fixed to them at the one end. The cables were at two different positive potentials operating against a common ground potential: one half at +28 V, the other at +50 V. The resistors were selected such that currents of ca. 2.5 A flow through each of the two circuits. All 5 cables on one potential were operated in parallel to facilitate the failure analysis after the tests. Each cable from the lower potential was twisted with a cable from the higher potential. The harness was manufactured by combining the 5 twisted pairs to one strand and fixing it with a cable binder to a bracket that was spaced 10 mm in front of the witness plate (Fig. 3). The harness strands are spaced 20 mm and wound 4 times to have better coverage of the fragment dispersion area.

The electrical set-up is shown in Fig. 4. Two power sources provide electrical power to the load resistors  $R_l$ . The section between the measurement resistors  $R_u$  and the load resistors  $R_l$  (i.e. the harness bundles) corresponds to the area where the impact occurs. The resistor  $R_x$  represents the resistance between the two conductors during and after impact when leakage currents and short currents are expected to flow across the junction. This set-up allows measurement of the resistance, voltages, and currents between the two cables and common ground.

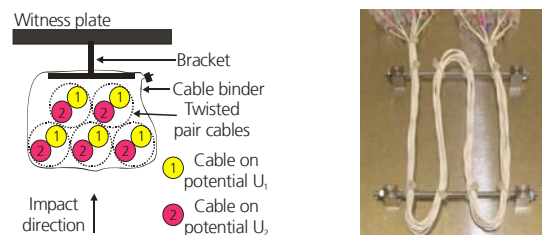


Figure 3. Cable set-up and fixation to witness plate

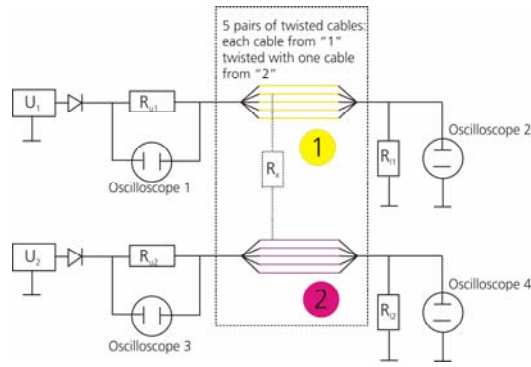


Figure 4. Electrical set-up for harness impact tests

All hypervelocity impact tests involving cloud conductivity tests and harness set-ups were performed in a vacuum of better than  $10^{-1}$  mbar, down to  $10^{-2}$  mbar (target chamber pressure). The ballistic limit tests were performed typically at target chamber pressures of 100 mbar, in some cases at chamber pressures down to 3 mbar.

### 3. SELECTED TEST RESULTS AND PRELIMINARY ANALYSIS

#### 3.1 Ballistic Limit Tests

Thus far 38 ballistic limit tests of the following CFRP H/C SPs have been performed: RAD1, RAD2, RAD3, GOCE, BEPPO-SAX. The impact conditions and coarse description of the results is provided in (Tab. 1). The failure criteria were defined in view of investigating the effects of contamination within the satellite interior:

- (1) Onset of electrical interferences is expected when spall detachment from the rear face-sheet of CFRP H/C SP occurs, hence defining the first failure criterion
- (2) Serious mechanical damages to equipment placed behind the satellite structure wall are expected when the rear face-sheet is completely perforated; this defines the second failure criterion.

For both criteria the threshold conditions are of interest and can be found for a selection of the configurations in Tab. 1. The projectile diameters which result in detached spall from the rear face-sheet of the CFRP H/C SP or any larger damage to the rear face-sheet are defined as the critical projectile diameters ( $d_c$ ). The  $d_c$  for all structures has been summarized in Tab. 2 over a range of impact angles and velocity regimes. In order to allow a quantitative comparison between the protection performances offered by the different CFRP H/C SPs tested in this campaign, the “normalized ballistic protection capability” (NBPC) was defined. This capability is the ratio of critical projectile diameter divided by the areal weight of the sample and is plotted in Fig. 5 for five different configurations impacted normally ( $0^\circ$ ) by projectiles with velocities exceeding 3

km/s. The plotted NBPC covers a range of values for each configuration. The NBPC is presented as a range given that the limited amount of impact tests performed during the test campaign does not allow exact determination of the failure criterion thresholds. However, it is fairly obvious that 4 out of 5 configurations have relatively the same normalized protection capability. The RAD1 configuration has a clearly lower protective capability. The main difference of the RAD1 structure to the other structures investigated is the thick honeycomb core (50.8 mm). Analysis is ongoing.

Table 1. Critical dia. ( $d_c$ ) ranges for CFRP H/C SP

Structure	$\alpha$ [°]	Velocity Regime [LV / HV]	$d_c$ between proj. dia. :
RAD1	0	LV	ca. 1.0
		HV	< 1.0
	45	HV	1.50 - 2.0
RAD2	0	HV	1.0 - 1.25
		HV	1.0 - 1.5
	45	HV	0.70 - 0.80
RAD3	0	LV	0.71 - 1.0
		HV	1.0 - 1.25
	45	HV	0.80 - 1.0*
GOCE	0	HV	1.0 - 1.55
	45	HV	1.0 - 1.5
SAX	0	HV	> 1.0
SAX	0	HV	0.80 - 1.0

NOTES:

- Velocity regime: LV ( $v < 3$  km/s), HV ( $v > 3$  km/s)
- Critical diameter defined for projectile which results in ANY contamination to the satellite interior (i.e. detached spallation and beyond).

\* A no-spall result was also obtained for 1.0 mm projectile diameter impact. However this test was performed at a reduced kinetic energy

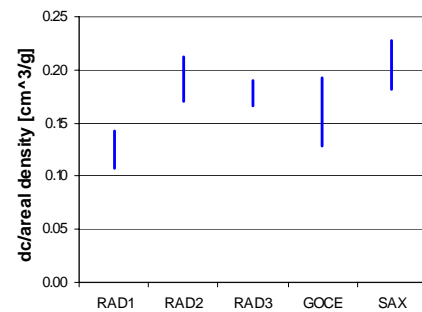


Figure 5. Normalized Ballistic Protection Capability of the tested CFRP H/C SP ( $0^\circ$  impact,  $3 < v < 7$  km/s)

Table 2. Ballistic Limit Tests of CFRP H/C SP and coarse test results description

Structure	EMI No.	v [km/s]	d <sub>p</sub> [mm]	α [°]	m <sub>p</sub> [mg]	E <sub>k</sub> [J]	Coarse result	Front FS [mm]		Rear FS [mm]	
								d <sub>h,ave</sub>	d <sub>sp</sub>	d <sub>h,ave</sub>	d <sub>sp</sub>
RAD1	B-107	2.02	1.25	0	2.9	2.9	NSP	2.3	5.0x4.7	No damage	
	B-106	2.36	1.0	0	1.3	1.8	SP	2.2	4.2x5.8	-	1.5x0.7
	B-164	3.13	1.5	0	5.61	27.4	P	4.29	7.9x4.7	3.6	7.4x6.5
	B-119	6.24	1.0	0	1.2	19.5	P	4.3	8.3x8.9	3.1	5.9x7.7
	B-117	6.27	1.0	0	1.2	23.6	P	4.5	8.6x7.6	1.1	5.6x4.2
	S-4577	5.72	1.5	0	5.4	88.3	P	5.74	8.5x10	6.42	9.9x11.3
	S-4578	5.72	1.5	0	5.4	88.3	P	6.07	7.2x9.8	5.96	11.1x11.7
	B-108	6.27	1.5	0	5.6	110.1	P	6.19	9.4x9.8	6.16	8.5x9.6
	B-161	4.27	1.0	45	1.52	13.9	NSP	3.2	6.5x6.2	No damage	
	B-167	3.39	1.25	45	2.87	16.5	NSP	3.5	6.4x8.3	No damage	
	S-4579	5.87	1.5	45	5.3	91.3	NSP	5.96	8.3x10.0	No damage	
	S-4580	6.12	2.0	45	11.8	221.0	SP	7.7	10.6x10.1	-	4.0x3.2
	S-4583	6.07	2.0	60	12	221.1	P	7.6	10.2x11.7	0.9	3.7x4.3
	S-4582	6.52	2.5	60	21	446.4	P	9.3	12.1x13.2	6.6	11.7x15.2
	S-4581	6.23	3.0	60	37.2	721.9	P	10.3	11.2x14.4	6.4	8.7x9.3
	RAD3	B-105	2.82	1.0	0	1.3	2.5	P	2.3	3.0x3.0*	1.5
B-139		3.36	1.0	0	1.51	8.5	P	2.3	3.7x2.5	1.0	1.9x4.1
B-127		5.88	0.50	0	0.4	6.9	NSP	1.5	3.3x2.0	No damage	
B-131		5.88	0.50	0	0.4	6.9	NSP	1.4	2.5x2.6+	No damage	
B-132		6.05	0.70	0	0.45	8.2	NSP	2.2	4.2x4.1	No damage	
B-154		5.94	0.80	0	0.31	16.1	SP	2.6	4.4x2.9	-	**
B-147		5.87	1.0	0	1.68	28.9	P	3.4	5.6x4.8	4.7	8.2x9.6
B-162		3.42	1.0	45	1.51	8.8	NSP	2.6	3.4x4.2	No damage	
B-140		3.33	1.25	45	2.92	16.2	SP	3.4	5.2x4.7	-	2.2x1.8
B-156		6.45	0.80	45	1.46	30.3	NSP	3.6	4.3x5.7	No damage	
B-133		6.18	1.0	45	1.44	27.5	SP	3.6	4.7x4.5	<0.5	3.5x2.7
B-160		6.62	1.0	60	2.05	44.9	NSP	3.8	4.5x5.8	No damage	
B-134		5.77	1.55	60	5.48	91.4	P	5.7	6.5x8.4	5.3	10.1x4.4
RAD 2	B-149	5.93	1.0	0	1.6	28.2	NSP	4.4	8.2x7.8	No damage	
	B-155	6.26	1.25	0	2.88	56.3	P	5.1	8.7x8.7	5.9	13.6x14.4
	S-4612	6.62	2.0	0	11.94	261.6	P	7.2	++	7.1	++
	B-150	5.96	1.0	45	1.56	27.7	NSP	4.5	7.0x8.1	No damage	
	S-4613	5.48	1.5	45	5.09	96.6	P	6.4	++	++	++
GOCE	B-146	5.98	1.0	0	1.57	28.1	NSP	3.7	30.1x39.0	No damage	
	B-152	6.26	1.5	0	5.85	114.6	P	6.5	29.0x28.7	5.5	57.9x61.8
	B-145	5.80	1.0	45	1.52	25.6	NSP	3.7	9.8x9.9	No damage	
SAX	B-153	5.94	0.80	0	0.91	16.1	NSP	3.1	3.6x8.3	No damage	
	B-148	5.96	1.0	0	1.52	27.0	P	3.4	4.4x8.8	4.3	13.6x46.5

+ Overlap of spall area from 2 tests. Average measurement taken

\* overlap from sabot part impact damage

\*\* was not be measured due to fabric protective layer on sample at time of shot

S- EMI Space Gun  
B- EMI Baby Gun

v impact velocity  
d<sub>p</sub> projectile diameter  
α impact angle

m<sub>p</sub> projectile mass  
E<sub>k</sub> kinetic Energy

d<sub>h,ave</sub> average hole dia.  
d<sub>sp</sub> spall diameter  
FS face sheet

NSP no spall  
SP detached spall  
P perforation (hole)

### 3.2 Cloud Conductivity Measurements

The set-up for cloud conductivity measurements allows the simultaneous investigation of mechanical impact damage to interior equipment and the electrical effects related to satellite interior contamination by conductive fibers. On the whole, about ten impact tests related to cloud conductivity measurements have been made so far of which one representative test result is analyzed in more detail here. The analysis concerns EMI Exp. S-4622 on a set-up involving a BEPPO-SAX CFRP H/C SP sample (Fig. 6). The impact conditions were 4.0mm/86.67 mg Al sphere,  $v = 6.64 \text{ km/s}$ ,  $\alpha = 45^\circ$ .

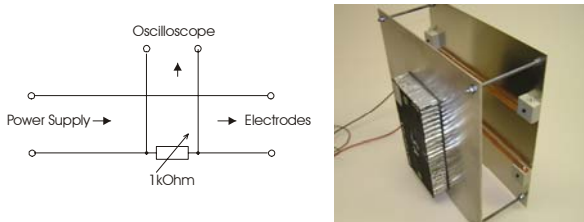


Figure 6. Complete target showing SAX CFRP H/C SP mounted on a frame and witness plate instrumented with electrodes

In Fig. 7, digital high-speed shadowgraph records of impact on the CFRP H/C SP, propagation of the fragment cloud, and impact of the cloud on the witness plate, is shown. As can be seen, there is considerable amounts of conductive fiber ejecta about the witness plate and therefore the electrodes.

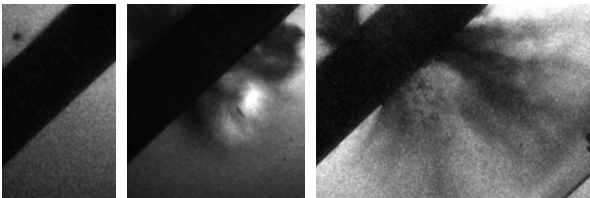


Figure 7. Optical Shadowgraphs of impact tests on SAX CFRP H/C SP with witness plate at a stand-off of 100 mm, EMI Exp. S-4622. Trigger times: 0, 20, 80  $\mu\text{s}$  wrt to first picture (4 mm Al-sphere,  $v = 6.64 \text{ km/s}$ ,  $\alpha = 45^\circ$ )

The actual impact damage in the witness plate is minor (Fig. 8): there are no impact craters observable, and the plate is covered extensively by Al-deposits over an area of approx. 150 mm x 110 mm, beginning about 50 mm above the witness plate center and some black dust stemming from CFRP fibers. The plate is not deformed, there is no noticeable bulging. Clearly the impulsive load transmitted to the plate is minor. However, the electrical signals obtained reveal intense electrical conduction between the electrodes during and after the cloud passage through the electrodes (Fig. 9).

Considering the electrical load resistor of 1 k $\Omega$  that is connected in parallel to the oscilloscope, currents of

several tens of milli-amperes flowing between the electrodes have been measured in this experiment, pulsating for a total duration of approximately 8 milliseconds after the impact. Based on the currents flowing between the electrodes and the applied voltage, the resistance between the electrodes was calculated to temporarily amount to below 50  $\Omega$ .



Figure 8. Impact damage in 1.5 mm thick witness plate after EMI Exp. 4622

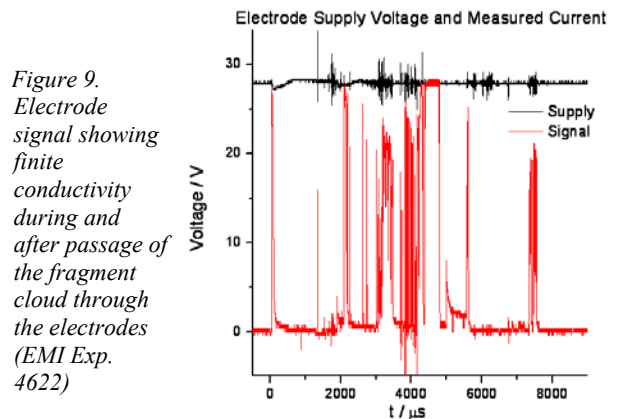


Figure 9. Electrode signal showing finite conductivity during and after passage of the fragment cloud through the electrodes (EMI Exp. 4622)

### 3.3 Harness Impact Tests

The set-up for harness impact tests allows for simultaneous measurement of fragment cloud mechanical impact damages, peak electrical voltages in cables, and leakage currents between the two circuits operated at different voltages. About 15 impact tests on harness set-ups have been performed so far, of which one representative result is analyzed in more detail in the following. The concerned hypervelocity impact test (EMI Exp. No. 4633) was on a RAD1 sample set-up with a cable harness located 100 mm behind the SP structure. The impact conditions were 5.0mm/176.6 mg Al-sphere,  $v = 6.81 \text{ km/s}$ ,  $\alpha = 0^\circ$ . The target set-up is shown in Fig. 10.



Figure 10. Complete target showing RAD1 CFRP H/C SP mounted on a frame holder and harness mounted on the witness plate

The digital high-speed shadowgraphs are displayed in Fig. 11. In Fig. 12 the mechanical damage of the cables is shown (3 cables were severed; 11 additional cables had the insulation removed/destroyed).

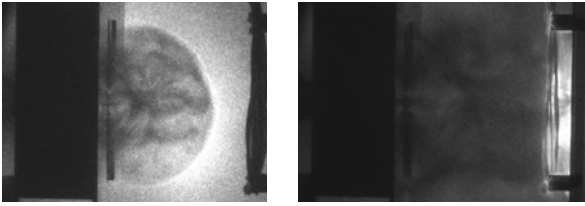


Figure 11. Optical Shadowgraphs of impact tests on RAD1 CFRP H/C SP with harness placed at a stand-off of 100 mm (+ witness plate behind), EMI Exp. S-4633. Trigger times: 10 and 20  $\mu\text{s}$  after impact ( $d=5\text{ mm}$ ,  $v=6.81\text{ km/s}$ ,  $\alpha=0^\circ$ )

Figure 12. Impact damage in cables and 1.5 mm thick witness plate (EMI Exp. 4633)



From the electrical measurements made during impact (Fig. 13), the potential difference between the cables operating at 28 V and those operating at 50 V was determined. This voltage should be constant if there is no conducting bridge between the circuits. Simultaneously, an electrical current flowing from one circuit into the other was measured, peaking at about 9 A. This indicates that the conductors from both circuits were in temporary contact during impact (ca.

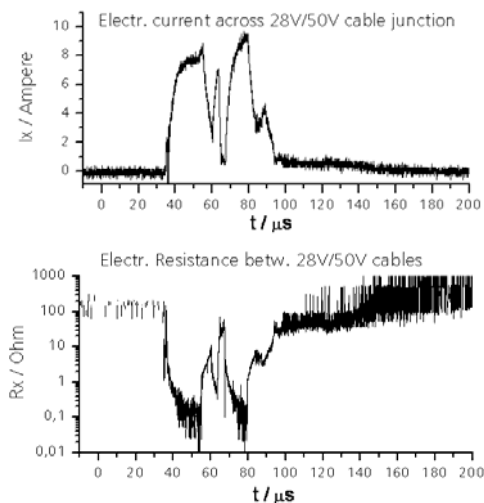


Figure 13. The current across the temporary junction between cables operated at 28 V and 50 V (top) indicates temporary contact between the conductors of both circuits. The electrical resistance (bottom) between the circuits was calculated from the measured potential difference between the circuits and the measured current (EMI Exp. 4633)

60  $\mu\text{s}$ ). From this information, the electrical resistance between the cables operated at 28 V and those operated at 50 V was calculated. As can be seen from the first plot in Fig. 13, the resistance approaches zero at approximately 53  $\mu\text{s}$  and 80  $\mu\text{s}$  after impact of the projectile on the CFRP front face-sheet. For reasons of amplifier noise and oscilloscope digitization in this plot 100  $\Omega$  resistance corresponds to “infinite resistance” i.e., no contact.

In Fig. 14, the voltage measured at the load resistor of the 28 V circuit are shown. The signals recorded during the first 100  $\mu\text{s}$  after impact reveal very high temporary voltage peaks (and associated current peaks). In the 28 V circuit, the voltage varies between 9 V and 58 V during impact of the main portion of the fragment cloud on the harness. In the 50 V circuit (not shown here), the voltage varies between 3 V and 67 V during the same time period. The duration of this large perturbation lasts for approximately 2  $\mu\text{s}$ . The subsequent smaller perturbations (in the order of  $\pm 15\text{ V}$ ) last several tens of  $\mu\text{s}$ .

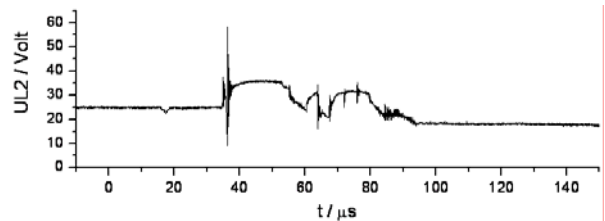


Figure 14. Voltage recorded in 28 V circuit during impact (EMI Exp. 4633)

#### 4. SUMMARY AND CONCLUSIONS

For five CFRP H/C sandwich panels, representative of satellite structure walls, ballistic limit data was obtained. Preliminary impact tests to investigate the secondary effects associated with perforation of the structure wall and associated ejection of conductive fibers into the interior of a satellite have been performed. It was found that large amounts of conductive fibers are ejected inside the satellite if the structure wall is perforated. Electrical shorts across electrodes that were mounted on witness plates located behind the CFRP H/C SP were measured. These shorts are caused by the conductive fibers. The duration of the measured shorts was in the order of milliseconds. For fragment cloud impact upon harnesses, large voltage peaks have been measured which drastically exceed the supply voltage. For cables at different electrical potentials, shorts and current flows have been measured indicating that severed cables (or cables with insulation removed) had electrical contact.

#### 5. ACKNOWLEDGEMENT

This study was performed under ESA/ESTEC Contract 16721/02.